

fluctuate less rapidly with time to be seen by the Mössbauer effect. The rising transmission seen above  $T_N$  may indicate a decrease in spin-fluctuation rates. However, local Co concentrations could also cause local increases in  $T_N$  such that the intensity curve looks like Fig. 14.

## VII. CONCLUSIONS

When NiO is doped with Co<sup>57</sup> under a CO<sub>2</sub> atmosphere, no trivalent contributions appear between 4.2 and 550°K. If the doping is done in air, a large portion of the Mössbauer  $\gamma$  intensity is in a trivalent Doppler spectrum. The trivalent Fe<sup>57</sup> is apparently caused by doping rather than charge relaxation.<sup>31</sup> Co prefers the trivalent state in the presence of oxygen. The trivalent

<sup>31</sup> W. Triftshauer and P. P. Craig, Phys. Rev. Letters 16, 1161 (1966).

state observed in Fe in MnO can probably be removed also by more careful preparation and doping.

The internal magnetic fields of divalent Fe reach a maximum and shrink as  $T$  is decreased when Fe is a dilute impurity in NiO, MnO, and CoO. This field dependence can be explained in detail by crystal-field theory for NiO and probably for MnO and CoO as well.

## ACKNOWLEDGMENTS

I wish to thank Professor J. G. Dash and Professor P. M. Higgs for their help and encouragement in making this work possible, and Dr. Charles S. Sahagian of the U. S. Air Force Cambridge Laboratories for supplying the NiO single crystal used in this work.

This work was supported by the U. S. Air Force Office of Scientific Research under Contract No. AF-AFOSR-594-64 and by the National Aeronautics and Space Administration under Grant No. Ns G 484.

# Fluorescence Studies of Energy Transfer between Single and Pair Cr<sup>3+</sup> Systems in Al<sub>2</sub>O<sub>3</sub>

RICHARD C. POWELL

*Air Force Cambridge Research Laboratories (OAR), Bedford, Massachusetts*

AND

B. DiBARTOLO,\* B. BIRANG,\* AND C. S. NAIMAN\*

*Miltras, Incorporated, Cambridge, Massachusetts*

(Received 25 July 1966; revised manuscript received 9 November 1966)

The fluorescence intensities and lifetimes of various no-phonon lines in ruby samples with 2.1 and 0.94% Cr<sup>3+</sup> were studied from 13 to 700°K. The temperature dependences of the intensities of numerous lines were used to determine the energy levels of two pair systems. The relative intensities of the single-ion ( $R$ ) lines and the pair ( $N$ ) lines are proportional to Boltzmann factors  $e^{-\Delta E/kT}$ , where  $\Delta E$  is the difference in energy of the metastable states, at high temperatures but not at low temperatures. The deviation from this law is greater and occurs at higher temperatures in the less concentrated sample. The fluorescence decays of the  $R$  and  $N$  lines are pure exponentials in the temperature region where the  $N$  lines follow a Boltzmann law; at low temperatures the  $N$  lines have an initial rise in fluorescence and then a decay. These results are interpreted in terms of coupled fluorescence systems consisting of single ions and pairs. A phonon-assisted cross-relaxation coupling process is suggested which allows for thermalization of the systems at high temperatures and direct pumping of the pair systems by the single-ion system at low temperatures. Energy transfer from single-ion to multi-ion systems was also observed.

## I. INTRODUCTION

WE have conducted an investigation of the effects of temperature on the fluorescence spectrum of dark ruby with two different concentrations of chromium. The fluorescence spectrum consists of two parts: (1) the sharp no-phonon lines due to pure electronic transitions, and (2) the broad "vibronic" bands due to vibrationally assisted transitions. The no-phonon lines of dark ruby can be classified as follows: the  $R_1$  and  $R_2$  lines due to transitions in the single-ion system, and the various satellite lines due to transitions in paired

Cr<sup>3+</sup> ions. These pair systems are formed by an exchange coupling between two Cr<sup>3+</sup> ions represented by the Hamiltonian  $JS_1 \cdot S_2$ .<sup>1,2</sup> The most prominent pair lines are designated<sup>3-5</sup>  $N_1$  and  $N_2$  and are, respectively, at 7041 and 7009 Å.

<sup>1</sup> A. L. Schawlow, D. L. Wood, and A. M. Clogston, Phys. Rev. Letters 3, 271 (1959).

<sup>2</sup> P. Kisliuk, A. L. Schawlow, and M. D. Sturge, in *Quantum Electronics III*, edited by P. Grivet and N. Bloembergen (Columbia University Press, New York, 1964), Vol. I, p. 725.

<sup>3</sup> It is the accepted usage to call the sharp lines next to the  $R$  lines on the long-wavelength side  $N$  (*Nebenlinien*) lines. See Refs. 4 and 5.

<sup>4</sup> H. du Bois and G. J. Elias, Ann. Physik 35, 617 (1911).

<sup>5</sup> O. Deutschbein, Ann. Physik 14, 712 (1932); 14, 729 (1932)

\* Supported by U. S. Air Force Contracts No. AF33(615)-2885 and No. AF33(615)-3985.

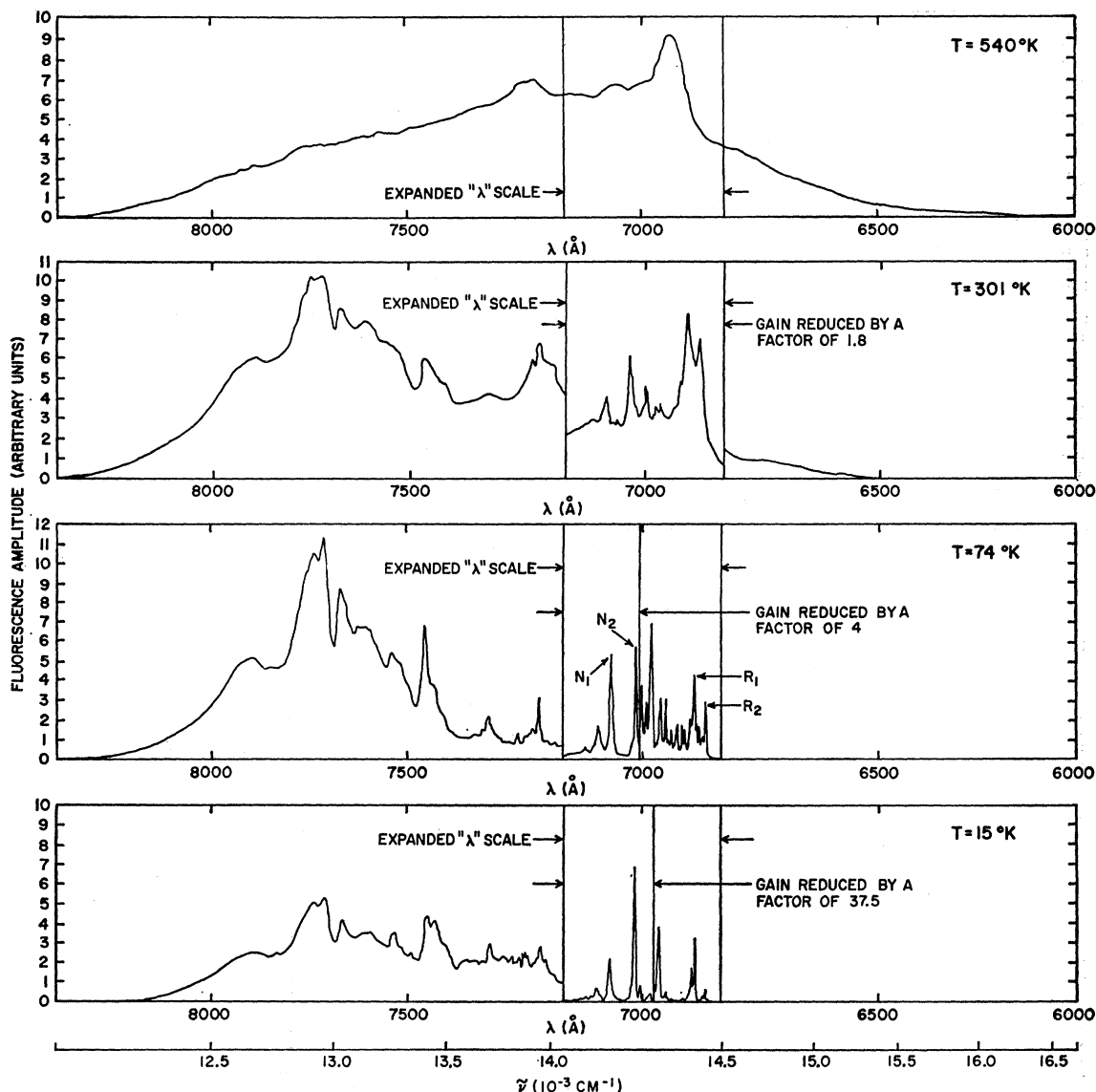


FIG. 1. Fluorescence of ruby with 2.1 at.% Cr.

The purpose of the present work was twofold: (1) the establishment of energy-level systems for  $\text{Cr}^{3+}$  pairs in ruby, and (2) the study of the interactions between single-ion and pair systems in the same crystal.

We have studied the relative intensities of all the no-phonon lines from 6900 to 7060 Å in samples with 2.1 and 0.94 at.% chromium at temperatures from 13 to 400°K. The resulting data were used to construct energy-level diagrams and to assign the various lines to specific transitions. The temperature dependence of the intensity ratios of  $R_1$ ,  $R_2$ ,  $N_1$ , and  $N_2$  lines yielded information about the energy transfer between single- and pair systems.

We have also measured the lifetimes associated with the  $R$  and  $N$  lines in the two samples at temperatures

from 13 to 700°K. The different temperature dependences of these lifetimes are consistent with the model used to explain the results of the relative intensity measurements.

For obtaining the intensities of the lines at various temperatures, each sample was mounted in a Janis Model 8DT cryostat and was excited by a General Electric BH6 1000-W air-cooled high-pressure mercury lamp. The fluorescence was observed at 90° to the direction of excitation, chopped, and focused onto the entrance slit of a Model 213 McPherson one-meter scanning monochromator. The direction of excitation and the direction in which the fluorescence was observed were both perpendicular to the  $c$  axis of the crystal. The signal was detected by an RCA 7102 (S-1) photo-

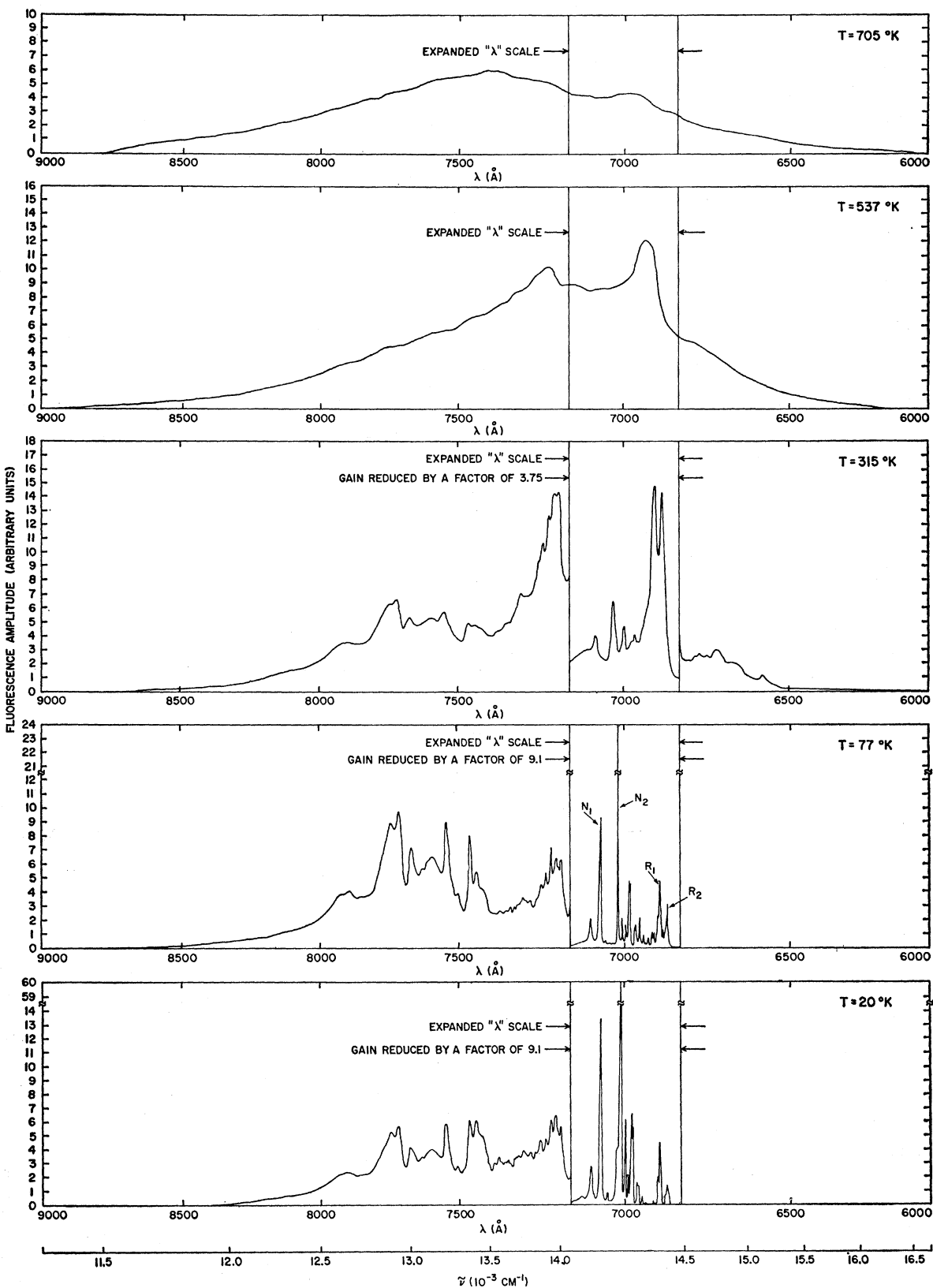


FIG. 2. Fluorescence of ruby with 0.94 at.% Cr.

multiplier tube cooled by liquid nitrogen, and amplified by a JB-5 Princeton Applied Research lock-in amplifier. The resolution of the apparatus was set at 0.3 Å for measurements used to establish the energy-level diagram; for studying the relative intensities of the  $R_1$ ,  $R_2$ ,  $N_1$ , and  $N_2$  lines, the resolution was set at approximately  $\frac{1}{10}$  of the linewidth.

For the pulsed fluorescence measurements, EG & G FX33 and FX12 flash tubes and the same monochromator were used; the fluorescence decay was observed and photographed in a Tektronix 531 scope. The time resolution of the apparatus was  $\sim 10$   $\mu$ sec.

## II. EXPERIMENTAL RESULTS

The complete unpolarized fluorescence spectrum at several temperatures is shown in Figs. 1 and 2 for the 2.1 and 0.94 at.% samples, respectively. At high temperatures, the spectral distribution of the energy is spread out over a wide region of low intensity. As the temperature is lowered, more of the energy is emitted in the no-phonon lines and less in the vibronic bands. The high-energy vibronics disappear at low temperatures because of the lack of phonons available for absorption. An intense band near 7750 Å, not present in pink ruby and attributed by Tolstoi *et al.*<sup>6</sup> to transitions involving more than two interacting chromium ions, appears in the fluorescence spectra.

It should be noted that the spectra as represented in the figures have not been corrected for photomultiplier response and grating efficiency. Taking these into account would cause the no-phonon lines to be slightly greater than they appear with respect to the large band at 7750 Å.

Figure 3 shows the portion of the spectrum consisting of the no-phonon lines at various temperatures. As temperature is lowered, the  $N_1$  and  $N_2$  lines increase in intensity, while the  $R$  lines decrease. Some other pair lines decrease in intensity as temperature is lowered, while a few others increase.

The relative intensities of all the no-phonon lines were measured at various temperatures. Of particular interest were the temperature dependences of the intensity ratios of the  $R_1$ ,  $R_2$ , and  $N_2$  lines to the  $N_1$  line and the intensity ratios of the  $R_1$  and  $R_2$  lines to the  $N_2$  line. These are shown in Fig. 4 for both the 2.1 and 0.94 at.% samples. The experimental data for each ratio can be fitted at high temperatures to an exponential  $e^{-\Delta E/kT}$ , where  $\Delta E$  is the difference in energy of the initial (metastable) levels of the two transitions involved. At low temperatures, the ratios deviate from this temperature dependence; the temperature at which this deviation occurs is greater for the less doped (0.94 at.%) sample. Also, the deviation from the exponential law at low temperatures is greater for this

TABLE I. Measured values of  $t_{\max}$ .<sup>a</sup>

Sample (at.% Cr)	$T$ (°K)	$t_{\max}$ ( $\mu$ sec)		
		$N_1$	$N_2$	7750 Å
2.1	10	110	70	30
	80	0	0	30
	300	0	0	0
0.94	15	270	260	Double decay
	77	250	250	
	102	140	100	
	112	140	0	

<sup>a</sup> Accuracy:  $\pm 20$   $\mu$ sec.

sample. The ratio  $I_{R_2}/I_{R_1}$  was observed to follow an exponential law even at low temperatures.

The fluorescence-decay times for the  $R$  and  $N$  lines were measured from 700 to 13°K and are reported in Fig. 5. In the temperature range where the intensity ratios follow the Boltzmann law, all the lines present purely exponential decays with the same time constants. For the 2.1 at.% sample, all the lifetimes coincide and increase from 0.04 msec at 700°K to 2 msec at 350°K and decrease as the temperature is lowered further. For the 0.94 at.% sample, all the lifetimes coincide and increase from 700°K to a maximum of 3.5 msec at 250°K and then decrease slightly as the temperature is lowered further. For the 2.1 at.% sample, the decay time of the  $R$  levels tends toward the value of 0.60 msec which is smaller than its intrinsic value of about 3.6 msec<sup>7</sup>; for the 0.94 at.% sample the decay time of the  $R$  levels tends toward the value 2.5 msec.

At temperatures lower than the one at which the deviation from the Boltzmann law occurs ( $\sim 70$ °K for the 2.1 at.% sample and  $\sim 90$ °K for the 0.94 at.% sample), the  $R$  lines continue to present purely exponential decays, whereas the  $N$  lines present an initial rise in the curves. The time  $t_{\max}$  at which the maximum occurs is given for the two  $N$  lines in the two samples in Table I. We notice that  $t_{\max}$  increases as the temperature is lowered and is larger for the 0.94 at.% sample. The lifetimes reported in Fig. 5 are the decay times of the tail of the fluorescence occurring after the initial rise. For the 2.1 at.% sample, the decay time of the tail coincides with the lifetime of the  $N$  lines ( $\tau_{N_1}=1.3$  msec,  $\tau_{N_2}=1.1$  msec)<sup>8</sup>; for the 0.94 at.% sample, this decay time coincides with the lifetime of the  $R$  lines.

The lifetime for the band at 7750 Å is shown in Fig. 6. Above 400°K, this lifetime coincides with that of the  $R$  lines. Below this temperature, a double decay is observed in the 0.94 at.% sample with the longer lifetime equal to that of the  $R$  lines. For the 2.1 at.% sample, an initial rise in the fluorescence is observed with the tail of the fluorescence showing a decay time equal to the lifetime of the  $R$  lines. Also, in this case

<sup>6</sup> N. A. Tolstoi, L. Shun<sup>2</sup>-fu, and M. E. Lapidus, Opt. i Spektroskopia **13**, 242 (1962) [English transl.: Opt. Spectry. (USSR) **13**, 133 (1962)].

<sup>7</sup> D. F. Nelson and M. D. Sturge, Phys. Rev. **137**, A1117 (1965).

<sup>8</sup> G. F. Imbusch, Quantum Electronics Conference, Phoenix, Arizona, April, 1966, Paper TB5 (unpublished).

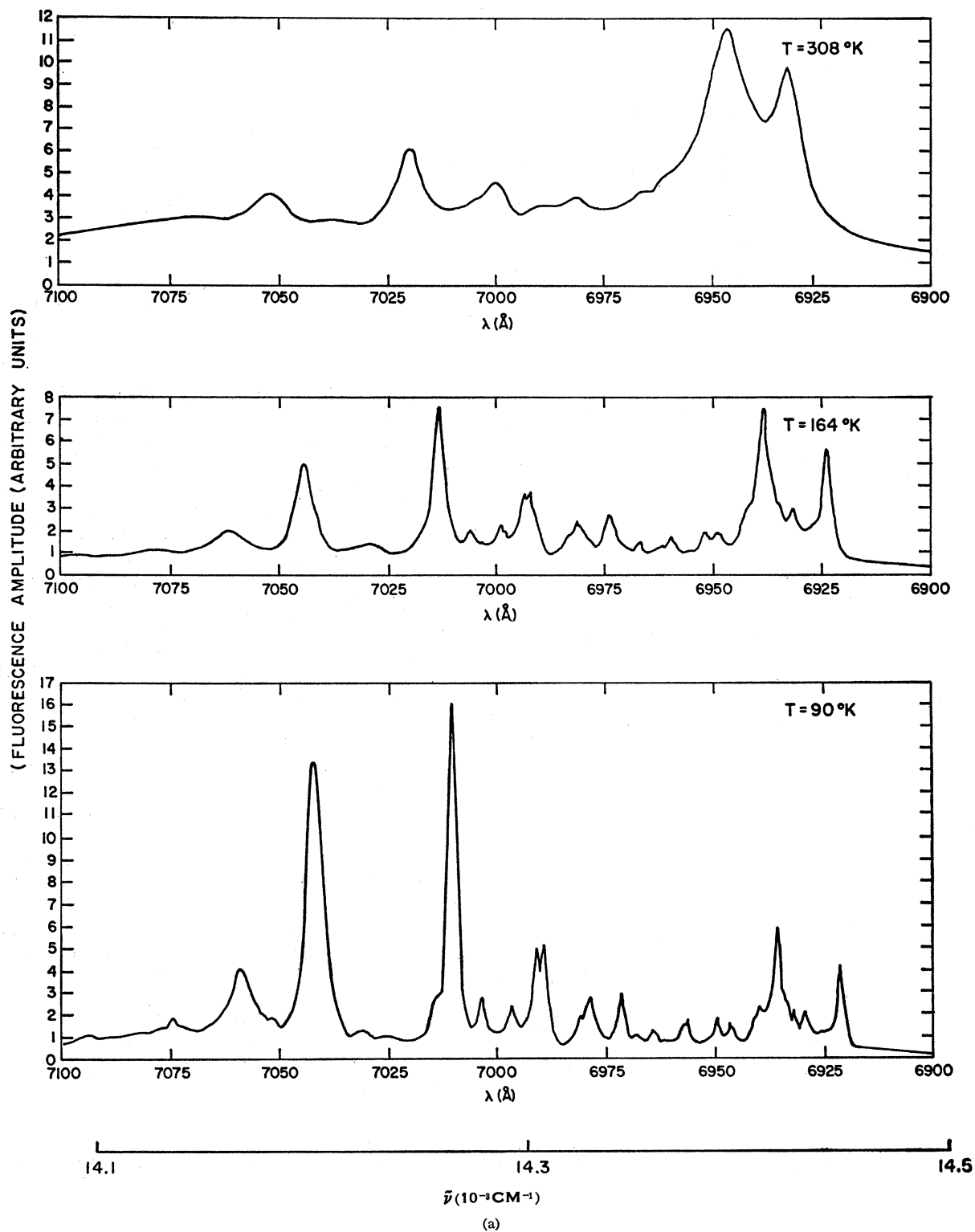
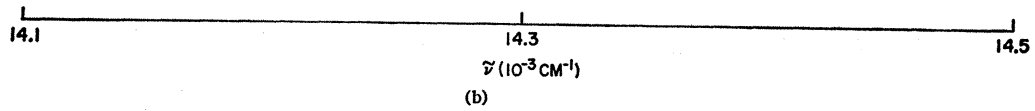
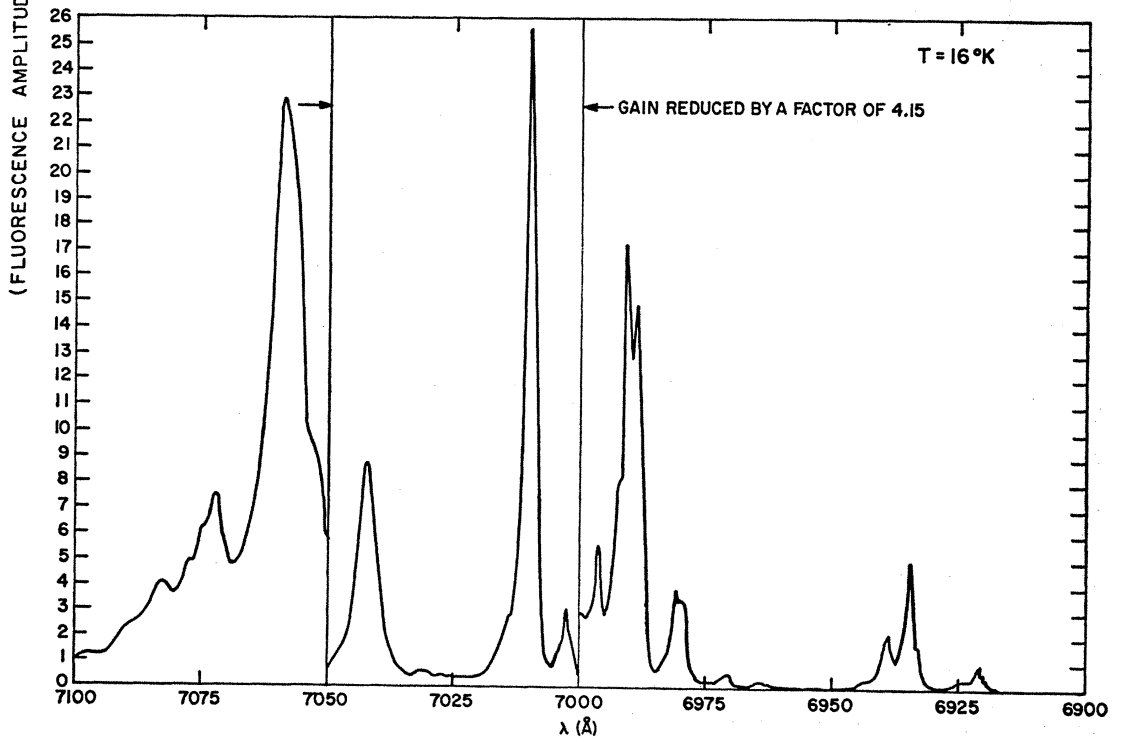
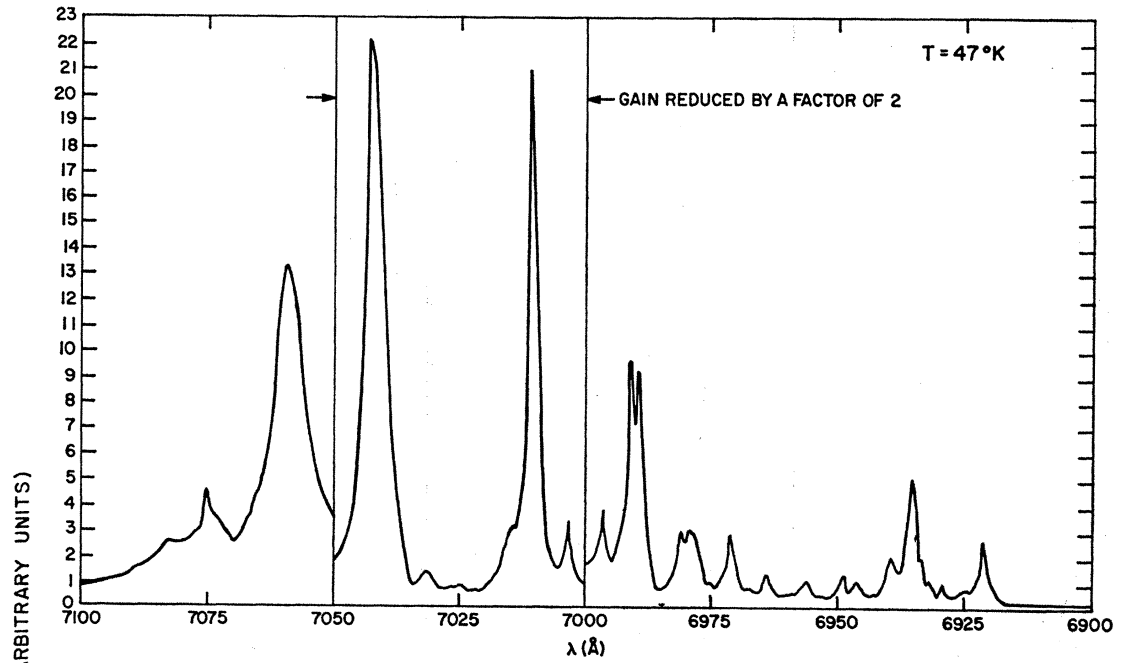


FIG. 3. Fluorescence of the no-phonon lines of ruby with 2.1 at.% Cr.



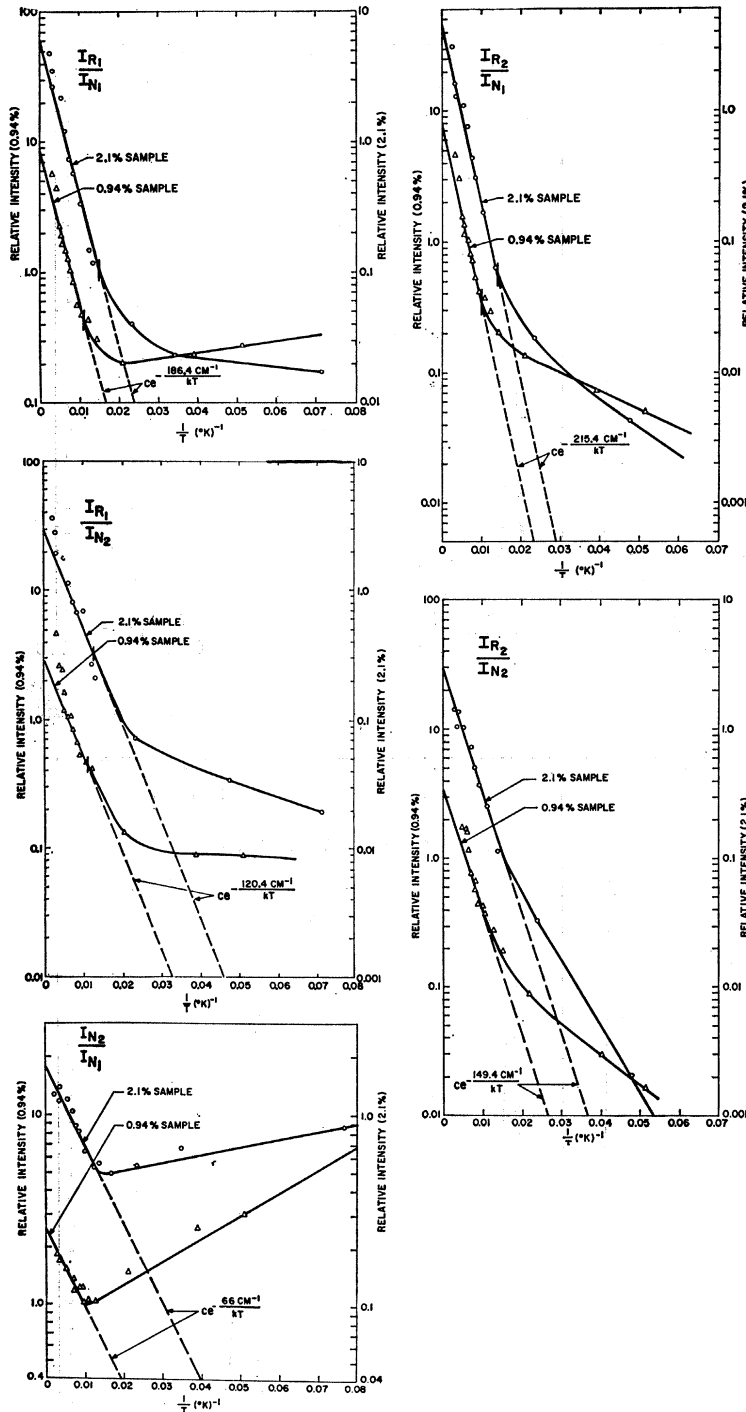


FIG. 4. Relative fluorescence intensities of the  $R$  and  $N$  lines in ruby with 2.1 and 0.94 at. % Cr.

$t_{\text{max}}$  increases as the temperature is lowered (see Table I).

### III. CONSTRUCTION OF THE ENERGY-LEVEL SYSTEMS AND ASSIGNMENT OF THE TRANSITIONS

The study of the concentration dependence of the intensities of the absorption lines appearing on the low-

energy side of the  $R$  lines in ruby led Schawlow and co-workers<sup>1,2</sup> to attribute these lines to transitions involving exchange-coupled pairs of chromium ions. From the temperature dependence of the strengths of the  $N_1$  and  $N_2$  lines in absorption, they determined the ground-state splittings and hence, by fitting to theory, the  $J$  values for two nonequivalent types of pairs. The  $N_1$  pairs were found to be antiferromagnetically coupled

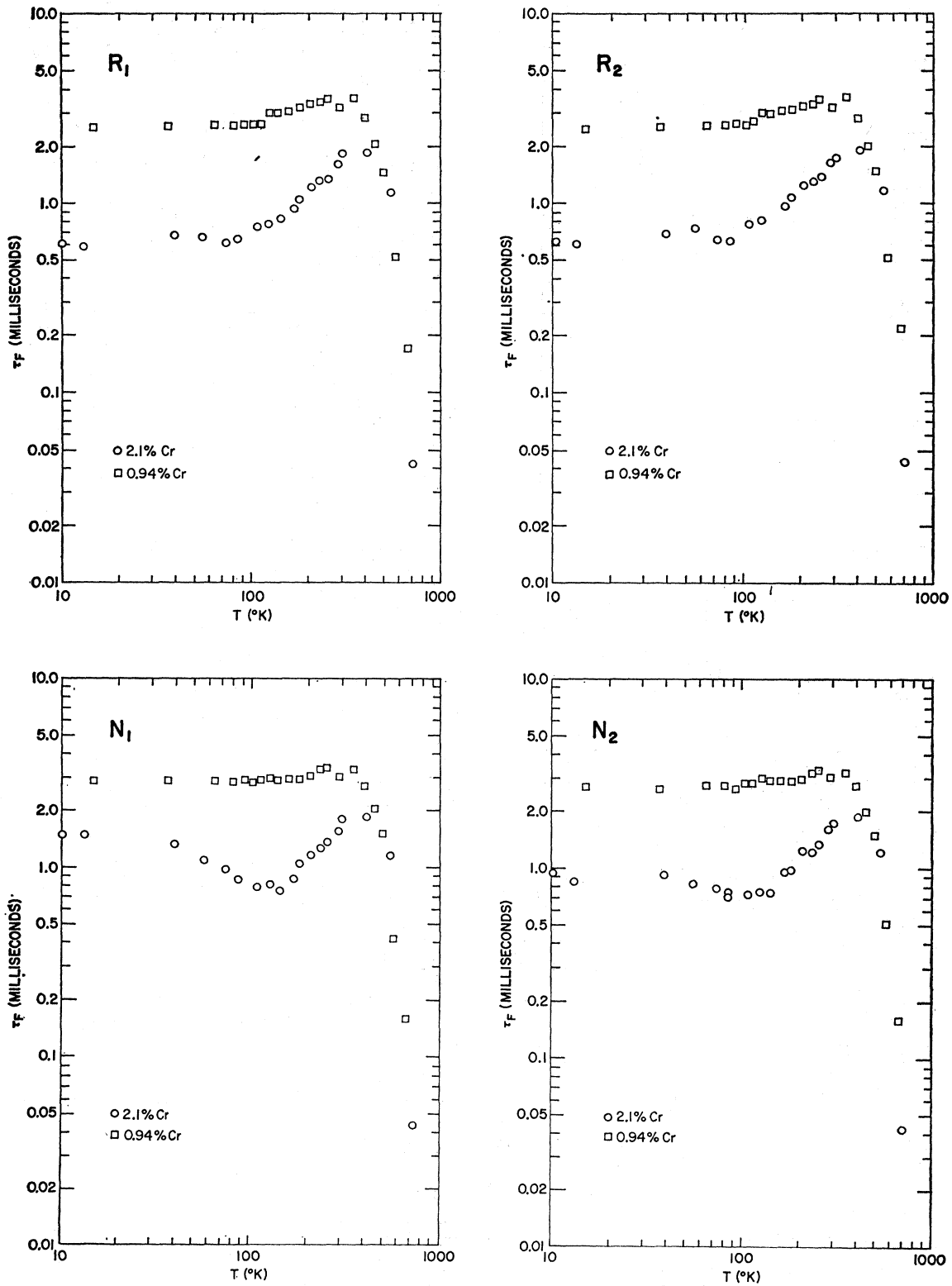


FIG. 5. Fluorescence lifetimes at the  $R$  and  $N$  lines of ruby with 2.1 and 0.94 at.% Cr. The  $R$  lines have pure exponential decays at all temperatures. The  $N$  lines have an initial rise in fluorescence and a subsequent decay at temperatures less than about 100°K for the 0.94 at.% sample and 70°K for the 2.1 at.% sample. The experimental points are the decay times of the curve after the initial rise.



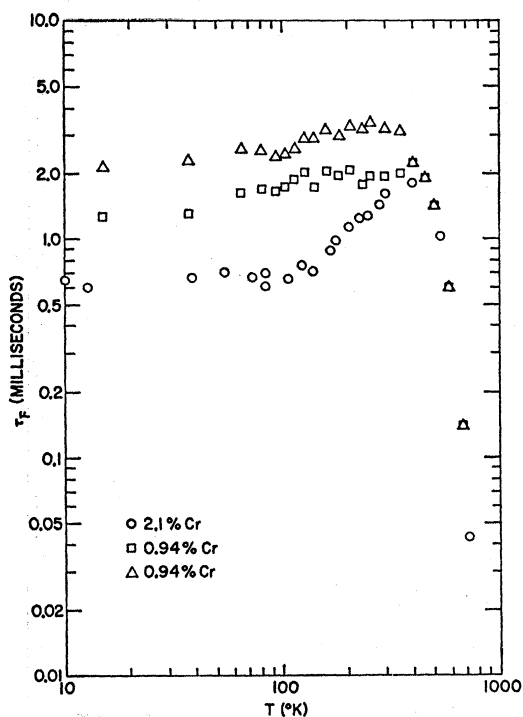


FIG. 6. Fluorescence lifetimes at the band near 7750 Å in ruby with 2.1 and 0.94 at.% Cr. Below about 300°K, the band in the 0.94 at.% sample has an initial fast decay and a subsequent slower decay. For the 2.1 at.% sample, the band has an initial rise in fluorescence below about 300°K; the experimental points are the decay times of the curve after the initial rise.

and the  $N_2$  pairs ferromagnetically coupled. Several other lines reported by Jacobs<sup>9</sup> were found to fit transitions between the  $N$  metastable levels and various components of the ground-state manifolds. Daly<sup>10</sup> attempted to determine some of the higher excited states by monochromatic excitation. Kisliuk and Krupke<sup>11,12</sup> used Daly's data and the recurrence of the previously established ground-state splittings to assign other observed lines to transitions involving upper levels of the excited manifolds. They also found improved values of the ground-state levels by including a biquadratic exchange term in the Hamiltonian.

From the measurements of the relative intensities of the fluorescence lines we were able to establish similar energy-level diagrams for the two pair systems and assign the observed lines to specific transitions. Two facts were used in interpreting the results of the relative-intensity measurements: (1) The intensities of the fluorescence lines originating from the same level have

the same temperature dependence, and (2) the intensities of the fluorescence lines originating from different levels in thermal equilibrium obey the relationship

$$I_1/I_2 = \text{const} \times \exp(-\Delta E_{12}/kT). \quad (1)$$

The results of these considerations are shown in Fig. 7.

Starting with the well-known  $R$ -line transitions, thermalization of relative intensities fixed the levels involved in the  $N_1$  and  $N_2$  transitions. These and other pair levels established by thermalization measurements are indicated by a  $T$ . Then lines with constant intensities relative to these lines established by thermalization were assigned to specific transitions. This fixed the ground-state levels marked with  $A$ . Three or more lines having the same temperature dependence and differing in energy by amounts equal to certain ground-state splittings were used to establish the excited states marked with  $B$ . A number of other observed lines which were not well enough resolved to obtain an accurate temperature dependence were assigned to specific transitions by considering their qualitative change with temperature and the established energy splittings. Our assignments, although used mainly on those lines whose temperature dependences we could measure accurately, put the previously given energy-level scheme on a much firmer ground.

The results obtained are consistent with those of Kisliuk and Krupke.<sup>12</sup> For the  $N_1$  pair we established four ground-state levels and four excited-state levels. Twelve lines were assigned to transitions between various sets of levels in this system. One of them, the 6978.4 Å line, was not assigned by previous workers.

The more closely spaced levels belonging to the  $N_2$  pair system made accurate intensity measurements more difficult for the corresponding lines. For this system, only three of the four levels of the ground state and three of the six levels of the excited state were firmly fixed. The other levels, established by Kisliuk and Krupke, are marked by  $K$ . Also, we assigned only 12 transitions within the  $N_2$  system where Kisliuk and Krupke assigned 18.

At least seven lines not assigned previously were observed near to the  $R$  lines. These lines are too closely spaced to obtain accurate intensity measurements. However, by virtue of their general change with temperature and their energy splittings compared to the ground states of the pair systems, it seems quite reasonable to assign at least three of these lines to specific transitions. These transitions established a new excited-state level in the  $N_2$  pair system which falls between the  $R_1$  and  $R_2$  metastable levels and is marked by a  $D$  in Fig. 7. This is consistent with Daly's<sup>10</sup> observation of fluorescence at the  $N_2$  line while exciting at a frequency between the  $R_1$  and  $R_2$  lines.

<sup>9</sup> S. F. Jacobs, Ph.D. thesis, Johns Hopkins University, 1956, (unpublished).

<sup>10</sup> R. T. Daly, Paper No. TB16, presented at the Optical Society of America Meeting in Pittsburgh, Pennsylvania, 1961 (unpublished).

<sup>11</sup> P. Kisliuk and W. F. Krupke, Appl. Phys. Letters 3, 213 (1963).

<sup>12</sup> P. Kisliuk and W. F. Krupke, J. Appl. Phys. 36, 1025 (1965).

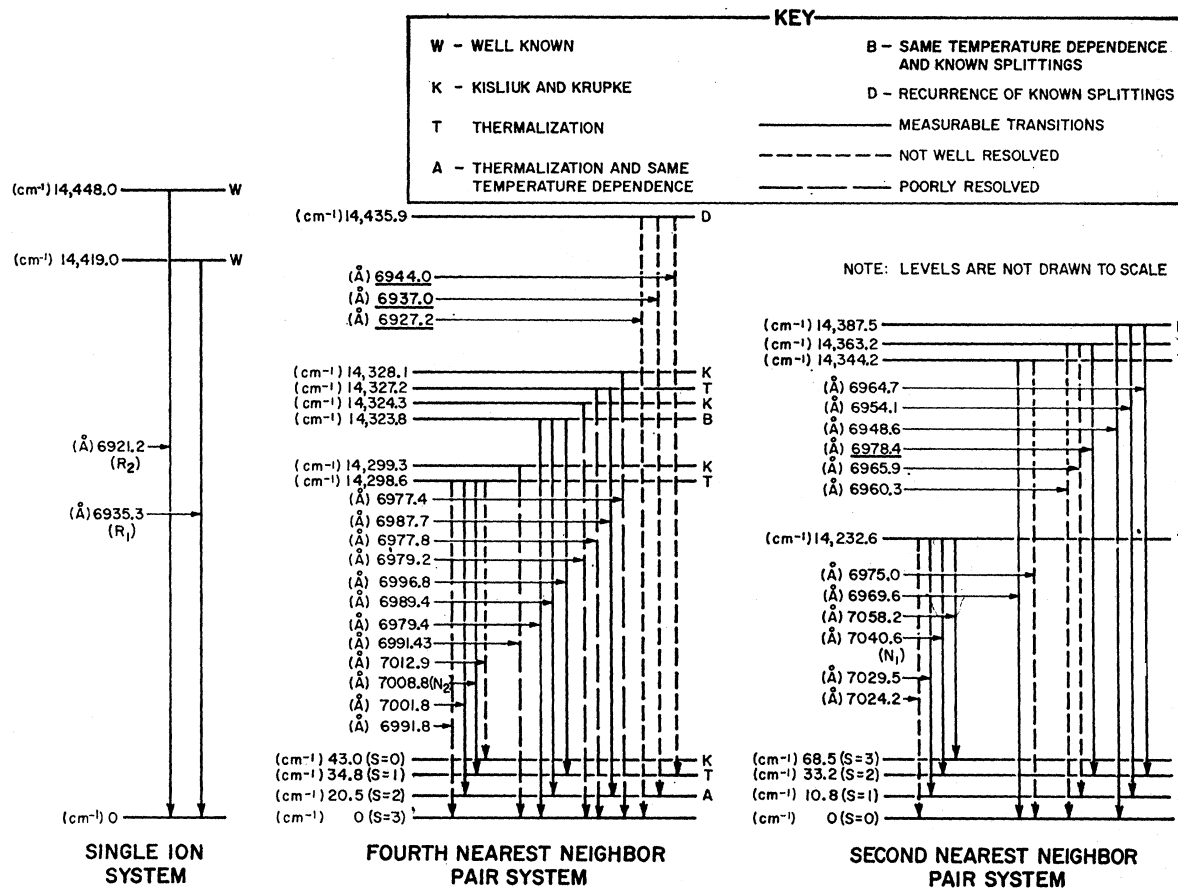


FIG. 7. Energy levels and transitions in the  $N_1$  and  $N_2$  pair systems established by relative-intensity measurements.

#### IV. ENERGY TRANSFER BETWEEN SINGLE-ION AND PAIR SYSTEMS: RELATIVE-INTENSITY MEASUREMENTS

Schawlow and co-workers<sup>1</sup> first suggested the presence of energy transfer from single ions to pairs, having observed that the increase in the relative intensity of the  $N_2$  line to the  $R_1$  line as a function of concentration was greater than linear above about 0.3 at. % chromium. Wieder and Sarles<sup>13</sup> excited a sample of heavily-doped ruby with the  $R_1$  emission of a ruby laser and observed the fluorescence in the  $N$  lines, thus explicitly demonstrating the energy transfer from single ions to pairs. Imbusch<sup>8</sup> investigated this energy transfer by measuring the fluorescence decays of the  $R$  and  $N$  lines. He concluded that the energy transfer comes from the main body of chromium ions and not just from the ions located near the pairs. He also found that this transfer becomes very efficient at concentrations of about 1.0 at. %  $\text{Cr}_2\text{O}_3$ .

We investigated the coupling of the single ion and pair systems by plotting the relative intensities of the

<sup>13</sup> I. Wieder and L. R. Sarles, in *Advances in Quantum Electronics*, edited by J. Singer (Columbia University Press, New York, 1961), p. 214.

$R$  and  $N$  lines at different temperatures, as shown in Fig. 4. These curves for the two samples are indicative of the temperature and concentration dependence of the energy-transfer mechanism. The fact that the departure from thermalization occurs at a higher temperature in the 0.94 at. % sample than in the 2.1 at. % sample and that for each line the amount of deviation from thermalization is greater in the less doped sample shows that the energy-transfer process is faster, relative to competing processes, in the more concentrated sample. The deviation from thermalization occurs at about 70°K for the 2.1 at. % sample and 90°K for the 0.94 at. % sample. The fact that the intensities of the lines within each pair system were observed to remain thermalized even at low temperatures gives additional evidence of the existence of separate systems.

One possible mechanism which can explain the observed characteristics of the energy transfer between the  $R$ ,  $N_1$ , and  $N_2$  systems is cross relaxation, which implies that a transition in one direction in one system is accompanied by a transition in the opposite direction in another system. Any energy mismatch of the two transitions can be balanced by phonon processes. The nature of this transfer mechanism has been investigated

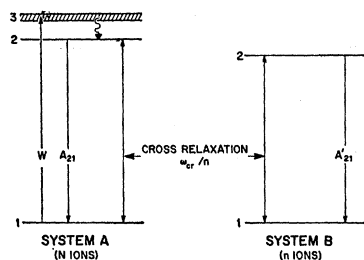


FIG. 8. Cross relaxation between two types of fluorescence systems.

by Imbusch,<sup>8</sup> who found some experimental evidence of its quadrupole-quadrupole character. Our experimental finding that the  $R$  and  $N$  levels are thermalized over a range of temperatures is an additional proof that the transfer is nonradiative.

Consider the simplified model of cross relaxation between two systems of ions shown in Fig. 8, where systems  $A$  and  $B$  represent the  $R$  and  $N$  systems, respectively. The rate equations for the populations of the various levels can be written as follows:

$$\begin{aligned}\dot{N}_2 &= WN_1 - A_{21}N_2 + n_2N_1\omega_{cr}'/n - N_2n_1\omega_{cr}/n, \\ \dot{N}_1 &= -\dot{N}_2, \\ \dot{n}_2 &= -n_2A_{21}' - n_2N_1\omega_{cr}'/n + N_2n_1\omega_{cr}/n, \\ \dot{n}_1 &= -\dot{n}_2.\end{aligned}\quad (2)$$

In the above equations, the assumptions have been made that the radiationless decay from the absorption band in system  $A$  to level 2 is extremely fast and that system  $B$  is pumped only through cross relaxation from system  $A$ . Cross relaxation between the two systems, in the simple scheme of Fig. 8, can take place only with the assistance of phonons of energy equal to the energy gap between level 2 of system  $A$  and level 2 of system  $B$ . Let us call this energy  $\Delta E_{22}$ . Because of the emission and absorption of phonons concurrent with the cross-relaxation, we may expect that

$$\omega_{cr}/\omega_{cr}' = e^{\Delta E_{22}/kT}.\quad (3)$$

Equations (2) and (3) can be solved, for the equilibrium conditions, with the assumptions that  $N_1 \approx N$  and  $n_1 \approx n$ ;

$$\begin{aligned}n_2 &= \frac{\omega_{cr}WN}{(A_{21}' + (N/n)\omega_{cr}') (A_{21} + \omega_{cr}) - (N/n)\omega_{cr}'\omega_{cr}}, \\ N_2 &= \frac{WN(A_{21} + (N/n)\omega_{cr})}{(A_{21}' + (N/n)\omega_{cr}') (A_{21} + \omega_{cr}) - (N/n)\omega_{cr}'\omega_{cr}},\end{aligned}\quad (4)$$

so that,

$$\frac{N_2}{n_2} = \frac{A_{21}'}{\omega_{cr}} + \frac{N\omega_{cr}'}{n\omega_{cr}}.\quad (5)$$

At high temperatures, the observed thermalization of the  $R$  and  $N$  levels, as in Fig. 4, implies that  $A_{21}' \ll \omega_{cr}'N/n$ . In Eq. (5), the second term is predominant, giving the experimental temperature de-

pendence of the  $I_R/I_N$  ratios. Equation (5) also predicts that  $N_2/n_2$  should be greater for the less concentrated sample; this concurs with the experimental results of Fig. 4.

At low temperature,  $\omega_{cr}'$  is expected to be very small and the first term in (5) is predominant. The temperature variation in this region may be considered to be due mainly to the variation of  $\omega_{cr}$ . The relevant times for the cross-pumping, as obtained by considering Fig. 4, are in the relation

$$\begin{aligned}\tau_{cr}(R_1 \rightarrow N_1) &> \tau_{cr}(R_1 \rightarrow N_2) > \tau_{cr}(R_2 \rightarrow N_1) \\ &> \tau_{cr}(R_2 \rightarrow N_2),\end{aligned}\quad (6)$$

where  $\tau_{cr}^{-1} = \omega_{cr}$ . The above relation implies that at low temperatures the  $N_1$  level is pumped less than the  $N_2$  level; this agrees also with the dependence of the  $I_{N_2}/I_{N_1}$  ratio with temperature (see Fig. 4). It also implies that the  $R_2$  level is pumping the  $N$  levels more efficiently than the  $R_1$  level. In the above considerations it is assumed that direct pumping of the  $N$  levels from the absorption bands<sup>14-16</sup> (for which decay measurements give evidence, as we shall explain later) affects the  $N$  levels by the same amount.

## V. ENERGY TRANSFER BETWEEN SINGLE-ION AND PAIR SYSTEMS: LIFETIME MEASUREMENTS

The lifetime measurements shown in Figs. 5 and 6 also yield information about the coupling of the single-ion and pair systems. All the lifetimes coincide with the intrinsic lifetime of the  $R$  levels<sup>7</sup> above 400°K where vibronic emission is the dominant decay mechanism. Below this temperature the lifetimes reach a maximum and begin to decrease while the  $R$ -line lifetime of pink ruby tends to become constant. For both samples, the lifetimes of the  $R$  and  $N$  levels coincide in the thermalization temperature range, as expected.

The lifetime of levels in thermal equilibrium is determined by the probabilities of natural decays of the levels, by their statistical weights, by their energy separations, and by the temperature. We do not know the statistical weights of the  $N$  levels, but, assuming them to be equal to those of the  $R$  levels, the lifetime for the coupled systems can be found from Eqs. (2) and (3) to be

$$\frac{1}{\tau_{R+N}} \propto \left( \frac{N_2}{\tau_R} + \frac{n_2}{\tau_N} \right) = N_2 \left( \frac{1}{\tau_R} + \frac{n_2}{N_2} \frac{1}{\tau_N} \right),\quad (7)$$

where  $N_2$  and  $n_2$  are, respectively, the populations of the  $R$  and  $N$  metastable levels. Note that in Eq. (7) the lifetime depends on concentration as well as tem-

<sup>14</sup> Excitation measurements indicate that fluorescence in the  $N$  systems takes place when the crystal is pumped in the single-ion absorption bands, with some evidence of optical pumping in a "pair" band at  $\sim 3400 \text{ \AA}$ . See Refs. 15 and 16.

<sup>15</sup> R. C. Powell, Ph.D. thesis, Arizona State University, 1967 (unpublished).

<sup>16</sup> A. Linz and R. E. Newham, Phys. Rev. **123**, 500 (1961).

perature. The intrinsic lifetimes of the  $N_1$  and  $N_2$  levels at 77°K are, respectively, 1.3 and 1.1 msec.<sup>8</sup> In the region between 400 and 100°K, these lifetimes will be even shorter. On the other hand, the  $R$  lifetime is larger and goes from 2 msec at 400°K to 4.2 msec at 100°K.<sup>7</sup> As the temperature is lowered,  $n_2$  increases and the lifetime of the coupled  $R+N$  states comes closer to the intrinsic values of the  $N$  states; this explains the decrease of the lifetime in the 400 to 100°K region (see Fig. 5). It also explains why the sample with less concentration has a smaller decrease after its maximum; this is because more of the population resides in the  $R$  levels in this sample than in the more doped sample.

The behavior of the lifetimes at temperatures lower than the one at which thermalization ceases may be explained by using the following rate equations, simplified from Eqs. (2) and (3) by letting  $\omega_{cr}'=0$ :

$$\begin{aligned}\dot{N}_2 &= -(\omega_{cr} + A_{21})N_2 + WN_1, \\ \dot{n}_2 &= \omega_{cr}N_2 - A_{21}n_2,\end{aligned}\quad (8)$$

where we have again used the approximation  $n_1 \approx n$ . Taking the time at the end of the exciting pulse to be  $t=0$ , for  $t>0$  we derive

$$\begin{aligned}N_2(t) &= N_2(0)e^{-p_3 t}, \\ n_2(t) &= \left[ n_2(0) + \frac{\omega_{cr}}{p_3 - A_{21}'} N_2(0) \right] e^{-A_{21}' t} \\ &\quad - \frac{\omega_{cr}}{p_3 - A_{21}'} N_2(0) e^{-p_3 t},\end{aligned}\quad (9)$$

where  $p_3 = \omega_{cr} + A_{21}$ . Two cases are of interest: initial rise and double decay.

#### A. Initial Rise

If the pulse is short enough, a maximum can occur for  $n_2(t)$  at a time  $t_{\max}$  after the end of the pulse given by

$$t_{\max} = \frac{1}{A_{21}' - p_3} \ln \left[ \frac{A_{21}'}{p_3} + \frac{A_{21}'(p_3 - A_{21}')}{p_3 \omega_{cr}} \frac{n_2(0)}{N_2(0)} \right]. \quad (10)$$

This time is related to the populations and probabilities as follows:

$$t_{\max} \geq 0 \quad \text{for} \quad \omega_{cr} N_2(0) / n_2(0) \geq A_{21}'. \quad (11)$$

#### B. Double Decay

$$A_{21}' > p_3, \quad n_2(0) > \omega_{cr} N_2(0) / (A_{21}' - p_3).$$

In this case, Eq. (9) reduces to the form

$$n_2(t) = A e^{-t/\tau_N} + B e^{-t/\tau_R}, \quad (12)$$

where  $\tau_N = (A_{21}')^{-1}$  and  $\tau_R = p_3^{-1}$  are the lifetimes of the  $N$  and  $R$  levels, respectively.

The lifetime of the  $R$  levels in the 2.1 and 0.94 at.% samples at low temperatures is shorter than its intrinsic

value. This fact is due to the presence of energy transfer even at low temperature, as confirmed by the smaller value that this lifetime has at high concentration. At high temperature, the cross-relaxation process is active only in creating a thermalization condition and the measured lifetime is the lifetime of the coupled systems. On the other hand, at low temperature, where the  $R$  and  $N$  systems are decoupled,  $\tau_R$  tends to  $(\omega_{cr} + A_{21})^{-1}$ , where  $\omega_{cr}$  now directly affects the lifetime. Disregarding reabsorption effects, the transfer efficiency at 10°K is about 80% for the 2.1 at.% ruby and about 20% for the 0.94 at.% ruby.

The behavior of the  $N$  decays at low temperatures, where an initial rise is observed, can be explained as due to the presence of the conditions of case *A* above. For both samples, using only the first term in the square bracket in (10), we find values for  $t_{\max}$  bigger (within one order of magnitude) than those given in Table I. The second term in the bracket is negligible on the assumption that the  $N$  levels are pumped only through the  $R$  levels. The consideration of the first term gives the right trends for the dependence of  $t_{\max}$  on temperature and concentration. However, to come closer to the experimental values, the second term in the bracket of (10) must be considered. The presence of direct pumping of the  $N$  levels from the absorption bands can actually make this term relevant, increasing the value of  $n_2(0)$ . We consider this as experimental evidence of the relevance of direct pumping of the  $N$  levels from the absorption bands.

For the band near 7750 Å, the decay times for both samples coincide with the decay times of the  $R$  and  $N$  lines in a thermalization range which extends from high temperatures to ~400°K. At lower temperatures in the 2.1 at.% sample, an initial rise in fluorescence is observed with the subsequent decay having the  $R$  lifetime. For the 0.94 at.% sample, a double decay is observed at the band with the longer decay time being equal to the  $R$  lifetime.

These results indicate that the initial level of the band is in thermal equilibrium with the initial levels of the  $R$ ,  $N_1$ , and  $N_2$  systems at high temperatures but not at low temperatures. The observed characteristics of the fluorescence decay fall into case *A* for the 2.1 at.% sample and into case *B* for the 0.94 at.% sample. For the 2.1 at.% sample (taking the shorter decay of the 0.94 at.% sample as the intrinsic lifetime of the band), the consideration of the first term in the bracket of (10) gives for  $t_{\max}$  a value ~30 times larger than the experimental value. This seems to imply that for the band the direct pumping from the single ion bands is very relevant at low temperatures. This is also in agreement with the fact that the band and the  $R$  systems decouple at higher temperatures than the  $R$  and  $N$  systems (see Figs. 5 and 6). As concentration decreases, the ratio  $N_2(0)/n_2(0)$  becomes larger, but  $\omega_{cr}$  for the  $R \rightarrow$  band transfer is smaller. Apparently, as concentration goes from 2.1 to 0.94 at.%, the de-

crease in  $\omega_{cr}$  exceeds the increase in the  $N_2(0)/n_2(0)$  ratio, shifting the conditions from case *A* to case *B*. A similar effect was found by Imbusch,<sup>8</sup> who observed a double decay for the *N* levels of a 0.2 at.-% ruby and, consistent with our measurements, a fluorescence rise for the same levels in a 1 at.-% ruby.

In the above considerations the effects of reabsorption on the relative intensities of the *R* and *N* lines have been neglected for a number of reasons.

(1) The temperature dependence of the  $I_{R_1}/I_{R_2}$  ratio shows that the intensities of the two *R* lines are exactly proportional, even at low temperatures, to the populations of the two corresponding metastable levels, implying that reabsorption does not affect their relative intensities.

(2) It is to be expected that reabsorption affects mainly the *R* lines relatively to the *N* lines, since the former, unlike the latter, terminate on the ground state<sup>17</sup>; moreover, reabsorption effects should be enhanced at low temperatures where the absorption lines become stronger and narrower. However, it is observed from the curves in Fig. 4 that the *R* lines do actually increase in intensity with respect to their thermalization values as the temperature is lowered below the critical value at which decoupling occurs.

(3) Actually, the deviations from thermalization of the intensity ratios are observed in a temperature region where reabsorption effects, if present, must be constant, since, in the same region, the  $R_1$  and  $R_2$  linewidths have been recognized to be independent of temperature.<sup>18</sup> Also, a "decoupling" effect may be observed for the  $N_1$  and  $N_2$  systems at low temperatures, as evidenced by the temperature dependence of the  $I_{N_1}/I_{N_2}$  ratio. (Again, the  $N_1$  and  $N_2$  lines are not significantly affected by reabsorption.)

(4) Finally, the behavior of the *R* and *N* line decays, which are the same at high temperature, but start to differ at the temperature at which thermalization ceases, is conclusive evidence that a decoupling effect is taking place.

<sup>17</sup> W. Jekeli, J. Opt. Soc. Am. **55**, 1442 (1965).

<sup>18</sup> R. C. Powell, B. DiBartolo, B. Birang, and C. S. Naiman, J. Appl. Phys. **37**, 4973 (1966).

## VI. SUMMARY

The investigation of the relative intensities and lifetimes of the *R* and *N* lines in heavily doped ruby gave the following results:

(1) The energy-level diagrams for the two established pair systems were constructed and numerous lines were assigned to the transitions between levels in these systems. These results were consistent with previous investigations, but one new level was established and four new lines were given assignments.

(2) The single-ion and the two-pair metastable levels were all observed to be in thermal equilibrium at high temperatures and to decouple at low temperatures. The temperature at which the levels decouple and the amount of deviation from thermalization were both greater for the less concentrated sample.

(3) A phonon-assisted cross-relaxation process was proposed as a mechanism for energy transfer between the *R* and *N* systems. In the scheme used, this process produces thermalization of the *R* and *N* levels at high temperature and allows continuous pumping from the *R* to the *N* levels at low temperature. It was also established that the pumping efficiency is greater for the  $N_2$  than for the  $N_1$  level and that pumping from the  $R_2$  level is greater than pumping from the  $R_1$  level.

(4) Lifetime measurements at the *R* and *N* lines and at the band near 7750 Å were consistent with the results of intensity measurements in that the decay times were observed to be the same at high temperatures but to differ at low temperatures. The observations of initial rises in fluorescence and double decays were indicative of the concentration dependence of the energy-transfer process. Rate equations were used to explain the results of the lifetime measurements. Evidence was given for the presence of a certain amount of direct pumping from the absorption bands to the *N* levels and to the band at 7750 Å.

## ACKNOWLEDGMENTS

The authors want to thank Dr. I. D. Abella for helpful discussions and Ray Tourtellot for his help with some of the calculations.